PHYSICAL REVIEW B VOLUME 42, NUMBER 4 1 AUGUST 1990

Inverse ac Josephson effect in long junctions

G. Costabile
Dipartimento di Fisica, Università di Salerno, I-84100, Salerno, Italy

R. Monaco and S. Pagano
Istituto di Cibernetica del Consiglio Nazionale delle Ricerche, I-80072 Arco Felice, Italy

G. Rotoli
Dipartimento di Fisica, Università di Salerno, I-84100, Salerno, Italy
(Received 5 December 1989; revised manuscript received 16 April 1990)

In highly hysteretic long Josephson junctions irradiated with microwaves the rf-induced current steps can cross the zero-current axis. The quantized voltage states arise from the phase locking of fluxon oscillations, which in rf-driven junctions can occur even with negative current bias. This phenomenon is interesting both for nonlinear dynamics and for application to the Josephson voltage standard.

The current-voltage (I-V) curve of highly hysteretic Josephson junctions irradiated with microwaves exhibits current steps which can cross the zero-current axis generating quantized voltage states in unbiased junctions. Following the suggestion of Levinsen *et al.*[1] this effect, known as the inverse ac Josephson effect, has been used to develop a Josephson voltage standard based on a large array of small junctions (i.e., junctions whose dimensions are much smaller than the Josephson penetration length λ_j) phase locked to an rf signal;[2] the dynamics of the phase and the stability of the phase locking in such junctions has been extensively investigated by Kautz.[3] There is experimental evidence of rf-induced steps[4] crossing the zero-current axis also in intermediate-length Josephson junctions; they occur when the frequency of the rf signal approaches the frequency of resonance of the junction. As the dynamics of the phase in long junctions irradiated by rf signals is very complicated, it has been investigated so far only either in the limit of small rf signals by numerical simulations and perturbative analytical approach[5-7] or in the limit of large rf signals by numerical simulation only.[8] In the first case, it has been shown that the oscillations of fluxons can be phase locked by the rf signal and that this event appears as a vertical straightening of the zero-field step (ZFS) in the current range where the phase locking occurs. In the second case, the stable configurations correspond to complex dynamical states producing quantized voltage steps; in these states at any instant the phase exhibits a spatial variation much larger than 2π within a fraction of the junction length. The spatial variation oscillates back and forth between the junction ends, while the phase generally advances in time at each point along the junction. This configuration should correspond to the experimental observation of high-order asymmetric current steps, growing from the McCumber curve.[9] In both cases the current at constant voltage is never zero. However, as was suggested by Chang[10] and Salerno *et al.*,[6] with a suitable choice for the rf amplitude, and with suitable junction parameters, the phase-locked oscillations of a fluxon can still take place even when the junction is biased with negative dc current. To investigate this point, we have performed numerical simulations that provide the configuration of the phase and its time evolution along a junction driven by an rf signal in a suitable range of parameters and we have also computed some I-V curves that are compared with the results of experiments.

The model equation is the perturbed sine-Gordon equation which describes the dynamics for the phase in a unidimensional junction having overlap geometry.[11] In normalized units

$$\phi_{tt}-\phi_{xx}+\sin\phi=\gamma_{\rm dc}-\alpha\phi_t+\beta\phi_{xxt}\,, \tag{1}$$

where $\phi(x,t)$ is the phase difference between the superconductive electrodes, $\gamma_{\rm dc}$ represents the constant dc bias current, assumed uniform throughout the junction, α is related to the losses in the tunneling barrier and β to the losses on the electrode surfaces, and subscripts denote partial derivatives. In Eq. (1) the lengths are normalized with respect to the Josephson penetration depth $\lambda_j=(\Phi_0/2\pi\mu_0 dJ_c)^{1/2}$, currents are normalized with respect to the junction critical current I_c, and time is normalized to the inverse of the plasma angular frequency $\omega_p=(2\pi J_c/\Phi_0 c_s)^{1/2}$, Φ_0 is the flux quantum, d is the junction magnetic barrier thickness, μ_0 is the vacuum permittivity, J_c is the Josephson current density, and c_s is the junction capacitance per unit area.

The rf electromagnetic field is introduced into this scheme through the boundary conditions[5-8]

$$\phi_x(0,t)+\beta\phi_{xt}(0,t)=\phi_x(l,t)+\beta\phi_{xt}(l,t)=\eta_0\sin\Omega t\,, \tag{2}$$

where η_0 is the amplitude of the rf field at junction ends normalized with respect to $\Phi_0/\mu_0\lambda_j d$.

We have integrated Eq. (1) for different values of the parameters using an explicit finite difference scheme; in this approach we discretize Eq. (1) in N spatial sections per unit length, obtaining an ordinary differential equation (ODE) system; in our simulations typically $N=40$. Then the ODE system was solved adopting the Bulirsch-Stoer algorithm with adaptive step size.[12] Initial condi-

tions were established following Erne and Parmentier.[13]

The experimental setup has been described in a previous paper.[4] The samples consisted of a Nb-Nb_xO_y-Pb overlap Josephson junctions, coupled to a microstrip line through a capacitive gap; the details of the geometry are show in Fig. 3 of Ref. 4. Table I summarizes the relevant parameters for the two samples measured at $T=4.2$ K. They have been evaluated from the I-V characteristic, from the pattern of the critical current, from the voltage of the Fiske steps, and from the maximum frequency of the signal emitted by the junction biased on the first ZFS. We recall that since the junction frequency of resonance is $f_r=\bar{c}/2L$ (where $\bar{c}=\lambda_j\omega_p$ is the velocity of the light in the junction barrier), then $2\pi f_r/\omega_p=\pi/l$.

Figure 1, relative to sample A, shows the I-V characteristic of the first ZFS as it is progressively modified by the increasing microwave power at about 11.2 GHz. Curve a refers to the unperturbed junction (i.e., no microwave applied), the successive curves exhibit the birth and the progressive growth of a straight, vertical current step that eventually takes the place of the original ZFS when the rf drive becomes sufficiently large. Each successive trace is offset in voltage by an amount proportional to the amplitude of the applied rf field. We remark that from curve c to curve f the vertical step crosses the zero current axis. The two lines clearly show the linear dependence of the phase-locked step amplitude on the externally applied microwave field. In Fig. 2 a similar behavior is shown for sample B, which has a larger normalized length (in this case the drive frequency is 15 GHz). In other words, we found that the inverse ac Josephson effect can be observed in junctions with any length. Also in this case the dependence of the phase-locked step on the rf field amplitude was found to be linear to a very high degree.

For the sake of comparison with the experimental data of Fig. 1, we report in Fig. 3 the result of the simulations describing the evolution of the first ZFS, obtained with $l=2.14$ and $\Omega=1.27$ (the normalized frequency of resonance in this case is $\pi/l=1.47$), and incrementing the amplitude of rf field by the same amount as in the experiment. Also here, successive traces are offset in voltage by an amount proportional to the rf field. We assumed as a reference level for the rf signal the amplitude that produced a step as large as step f in Fig. 1. The choice of the dissipation parameter α was the result of a tradeoff between computational efficiency and realism: the dissipation due to quasiparticle tunneling in real junctions is very low, but the lower α is in the model, the higher N must be to prevent numerical instability. The value of β was chosen to reproduce the experimental height of the first ZFS in the undriven junction, as this parameter appears[11] to determine the switching from the fluxon state to the

TABLE I. Geometrical and electrical (at 4.2 K) parameters of our samples.

Data	Sample A	Sample B
Length L (μm)	450	400
Width W (μm)	55	45
Critical current I_c (mA)	1.25	19.2
Josephson length λ_j (μm)	210	45
Plasma frequency f_p (GHz)	8.75	49.5
Resonant frequency f_r (GHz)	12.8	17.5
Normalized length l	2.14	8.9
Shunt loss α	0.02	0.025
Surface loss β	0.01	0.002

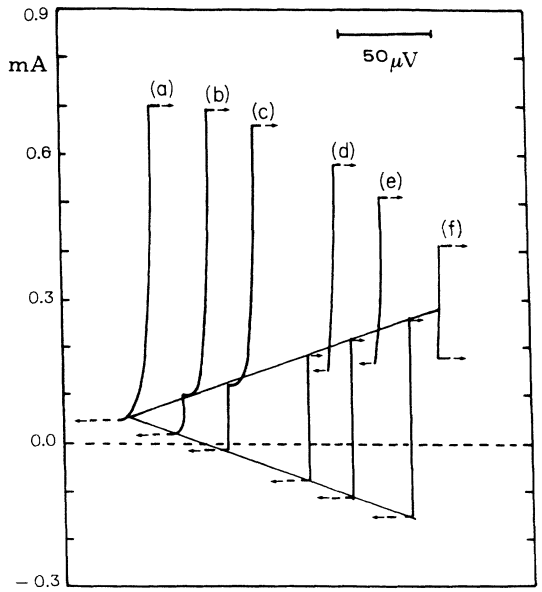

FIG. 1. Effect on the first ZFS of an increasing-amplitude microwave drive relative to sample A driven at 11.2 GHz; the rf power level (in dBm at the output of the rf generator) is (a) $-\infty$, (b) -50, (c) -45, (d) -40, (e) -38, and (f) -36. For clarity each successive trace is offset in voltage by an amount proportional to the amplitude of the applied rf field and straight lines help to show the linear dependence of the phase-locked step height on the rf drive amplitude.

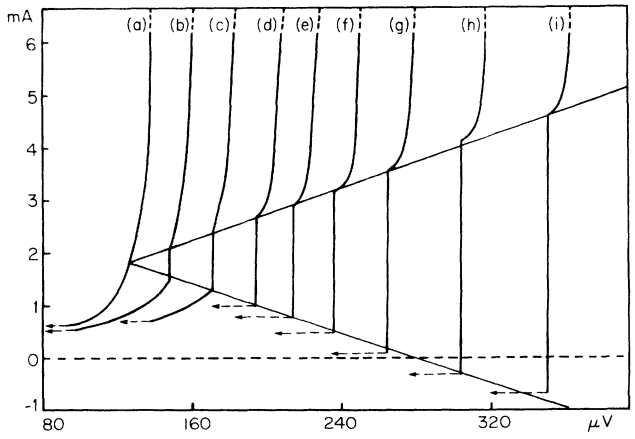

FIG. 2. Effect on the first ZFS of an increasing-amplitude microwave drive relative to sample B driven at 15.0 GHz; the rf power level (dBm at the output of the rf generator) is (a) $-\infty$, (b) -20, (c) -14, (d) -10, (e) -8, (f) -6, (g) -4, (h) -2, and (i) 0. For clarity each successive trace is offset in voltage by an amount proportional to the amplitude of the applied rf field and the straight lines help to show the linear dependence of the phase-locked step height on the rf drive amplitude.

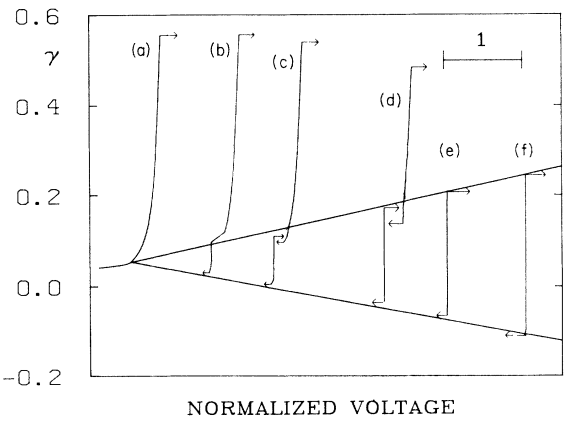

FIG. 3. The first ZFS calculated from Eq. (1) with $\alpha=0.02$ and $\beta=0.01$. The amplitudes of the rf field η_0 are (a) 0, (b) 0.1, (c) 0.18, (d) 0.32, (e) 0.4, and (f) 0.5 and correspond to the rf amplitudes of Fig. 1. For clarity each successive trace is offset in voltage by an amount proportional to η_0. The straight lines help to show the linear dependence of the phase-locked step height on the rf drive amplitude.

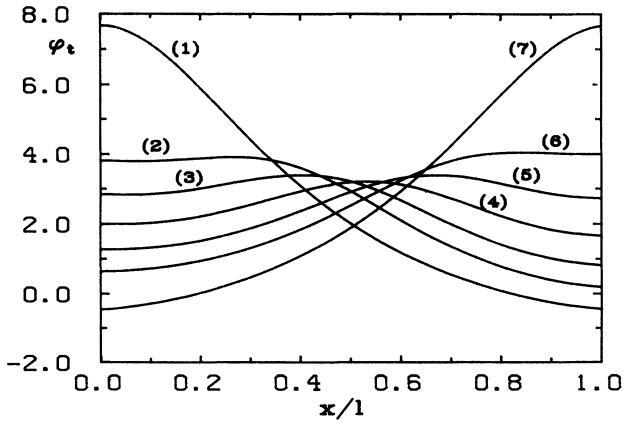

FIG. 4. The phase derivative along the junction at successive times, equally spaced by $T/12$, calculated at zero current bias on the phase-locked step. From (1) to (7) the plots cover a semiperiod of the fluxon oscillation relative to curve (f) of Fig. 1. The parameters are the ones of sample A with $\eta_0=0.5$, $\Omega=1.27$.

McCumber curve. For each value of γ, which was varied in steps of 0.0005, the numerical simulation provided the phase and the voltage along the junction at successive time intervals of about 0.05; in order to reconstruct the I-V characteristic from the numerical data, the voltage has to be time averaged. In Fig. 3, curve a is the current branch of the I-V characteristic corresponding to the first ZFS of the undriven junction generated by the fluxon oscillation. The next curves b-d are interpreted as in Refs. 6 and 7: the straight segment is a consequence of the phase locking of fluxon oscillations to the external drive and the locking range increases from left to right as the rf level is increased; the hysteresis can be ascribed to the low dissipation.[5] Therefore the curves in Fig. 3 are the dc counterpart of the experiment described by Cirillo and Lloyd,[14] who reported that the frequency of the radiation emitted by a long junction can be pulled and locked by an external rf drive. Curves e and f appear as straight, vertical steps (the small undulations are an artifact of the averaging algorithm) which cross the zero axis to a considerable extent. We have focused our attention on the dynamics of the phase at the zero crossing point of the last curve. A family of plots of the voltage configurations at successive time intervals is shown in Fig. 4. The dynamics can be interpreted as consisting of fluxon oscillations that are phase locked to the rf drive, as we checked inspecting how the voltage at a fixed point in the junction is related to the phase of the rf signal.[8] Because of the modest length of the junction and to the relatively large distance of the drive frequency from the ZFS resonance frequency, the spatial phase variation is smeared out over a large fraction of the junction. The solitonic aspect of the oscillation becomes more evident if we look at the phase configuration of a junction with larger normalized length. This effect is clearly shown in Fig. 5, where the parameters are those of sample B in Table I and $\gamma_{dc}=0$.

Previous perturbative analytical approaches[6,7] predict a linear dependence on the driving field amplitude, and are confirmed by our simulations which include surface impedence effects, as is shown by the two lines in Fig. 3.

The occurrence of quantized voltage states at zero current bias in junctions for which $L>\lambda_j$ is a phenomenon of interest for the Josephson voltage standard. Inasmuch as the dynamics of the phase differs considerably from the dynamics of the Shapiro steps, the stability criterion discussed in Ref. 3 is no longer valid. We did find, indeed, testing several samples, that the steps we are dealing with were stable in a relatively large frequency range near the plasma frequency where chaotic behavior is often observed in small junctions, and this fact could eliminate the need to drive the voltage standard device at mm wavelengths. Moreover, the rf-induced steps in long junctions can have typical amplitudes of a few hundreds μA, as is evident in Figs. 1 and 2, and therefore they are less sensitive to external noise. As a further remark, we also emphasize that the maximum quantized voltage that

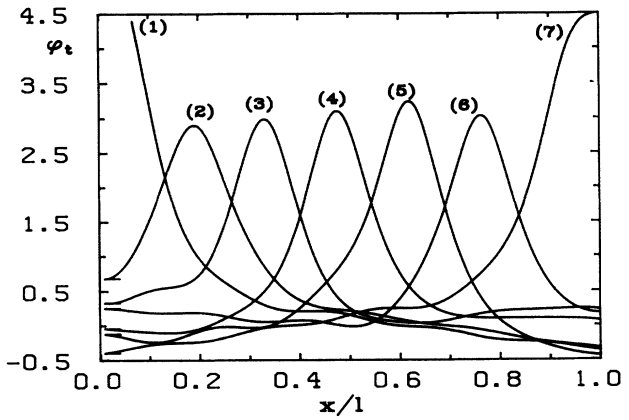

FIG. 5. The phase derivative along the junction at successive times, equally spaced by $T/12$, calculated at zero current bias on the phase-locked step. From (1) to (7) the plots cover a semiperiod of the fluxon oscillation. The parameters are those of sample B with $\eta_0=0.4$, $\Omega=0.30$.

can be obtained in a long junction with zero-current bias is much larger than the maximum voltage of the ZFS's. In fact, from Fig. 6 of Ref. 4 it can be seen that, operating in the X band with a junction having $l=2.1$ and the highest ZFS at 70 μV, the rf-induced steps cross the zero bias axis up to 300 μV. In the case of high order, all positive (i.e., not zero-crossing) steps numerical simulations have shown[8] that the dc current bias and the rf-drive play, to some extent, two different roles: the former mostly feeds a spatially uniform advancing of the phase while the latter is mostly responsible for the spatial phase variation along the junction. We suggest that this picture might also apply to the high-order zero-crossing steps, i.e., we think that the quantized voltage states of these steps at zero current bias arise principally from multiple fluxon oscillations in the junction. We intend to investigate the validity of this hypothesis in order to clarify the dynamics of the long Josephson junction also in this respect.

We are pleased to acknowledge fruitful discussions with R. D. Parmentier. We are grateful for the financial support received from the European Economic Community through Contract No. St-2-0267-J-C(A), from the Progetto Cray, and the Italian National Research Council under the Progetto Finalizzato "Superconductive and Cryogenic Technology."

[1]M. T. Levinsen, R. Y. Chiao, M. J. Feldman, and B. A. Tucker, Appl. Phys. Lett. **31**, 776 (1977).

[2]F. L. Lloyd, C. A. Hamilton, J. A. Beall, D. Go, R. H. Ono, and R. E. Harris, IEEE Electron. Dev. Lett. **EDL-8**, 449 (1987).

[3]R. L. Kautz, in *Structure, Coherence and Chaos in Dynamical Systems,* edited by Peter L. Christiansen and R. D. Parmentier (Manchester Univ. Press, Manchester, 1989), pp. 207–226.

[4]G. Costabile, R. Monaco, and S. Pagano, J. Appl. Phys. **63**, 5406 (1988).

[5]A. Davidson and N. F. Pedersen, Appl. Phys. Lett. **55**, 1132 (1989).

[6]M. Salerno, M. R. Samuelsen, G. Filatrella, S. Pagano, and R. D. Parmentier, Phys. Rev. B **41**, 6641 (1990).

[7]J. J. Chang, Phys. Rev. B **34**, 6137 (1986).

[8]G. Rotoli, G. Costabile, and R. D. Parmentier, Phys. Rev. B **41**, 1958 (1990).

[9]R. Monaco, S. Pagano, and G. Costabile, Phys. Lett. A **124**, 523 (1987).

[10]J. J. Chang, Phys. Rev. B **38**, 5081 (1988).

[11]S. Pagano, Ph.D. thesis, Technical University of Denmark, 1987 (unpublished).

[12]W. H. Press, B. P. Flannery, S. A. Teukolsky, and W. T. Vetterling, *Numerical Recipes* (Cambridge Univ. Press, Cambridge, 1986), Chap. 15.

[13]S. Erne and R. D. Parmentier, J. Appl. Phys. **52**, 1091 (1981).

[14]M. Cirillo and F. L. Lloyd, J. Appl. Phys. **61**, 2581 (1987).